Growing land-sea temperature contrast and the intensification of Arctic cyclones

Article

Published Version

It is advisable to refer to the publisher's version if you intend to cite from the work. See Guidance on citing.

To link to this article DOI: http://dx.doi.org/10.1029/2018GL077587

www.reading.ac.uk/centaur

CentAUR

Growing Land-Sea Temperature Contrast and the Intensification of Arctic Cyclones

Jonathan J. Day[1,2] 🆔 and Kevin I. Hodges[1]

[1]Department of Meteorology, University of Reading, Reading, UK, [2]Now at European Centre for Medium-Range Weather Forecasts, Reading, UK

Abstract Cyclones play an important role in the coupled dynamics of the Arctic climate system on a range of time scales. Modeling studies suggest that storminess will increase in Arctic summer due to enhanced land-sea thermal contrast along the Arctic coastline, in a region known as the Arctic Frontal Zone (AFZ). However, the climate models used in these studies are poor at reproducing the present-day Arctic summer cyclone climatology and so their projections of Arctic cyclones and related quantities, such as sea ice, may not be reliable. In this study we perform composite analysis of Arctic cyclone statistics using AFZ variability as an analog for climate change. High AFZ years are characterized both by increased cyclone frequency and dynamical intensity, compared to low years. Importantly, the size of the response in this analog suggests that General Circulation Models may underestimate the response of Arctic cyclones to climate change, given a similar change in baroclinicity.

Plain Language Summary The dramatic reduction in Arctic summer sea ice has led to an increase in human activity and hence exposure to extreme events in the Arctic. Unlike the midlatitude storm tracks, which are most active in winter, the Arctic storm track is most active in summer, exactly during the time when shipping and tourism are on the rise, leading to the obvious question of how climate change is affecting and will affect the storms themselves. Unfortunately, according to previous research by ourselves and others, climate models perform poorly in representing even the basic features, such as the summer maximum in Arctic cyclone frequency. As a result their projections for how Arctic cyclones will change in the future cannot be considered reliable. In this paper we use a new analog approach to assess the impact of a warming Arctic, using the observed record. By comparing statistics for years with high land-sea thermal contrast against years with low, we demonstrate that storms over the Arctic Ocean will likely become more frequent and more dynamically intense as the climate warms, increasing the risk to shipping and other human activities.

1. Introduction

As the seasonal progression into spring and summer months sees sunlight return to the Arctic, the high-latitude continents warm much faster than the Arctic Ocean, due to their lower heat capacity (Reed & Kunkel, 1960). This leads to large land-sea temperature contrasts and high levels of baroclinicity along the Arctic coastline (Figure 1a). As a result of vertical mixing of warm air over land, this band of strong temperature gradients extends through the troposphere (Crawford & Serreze, 2014; Serreze, Lynch, & Clark, 2001), see Figure 4a. This semi-permanent baroclinic region, known as the Arctic Frontal Zone (AFZ; 65–77°N, 50–260°E; Figure 1a), plays an important role in maintaining high levels of Arctic cyclone activity in summer (Crawford & Serreze, 2016; Serreze, 1995; Serreze & Barrett, 2008). As a result, the Arctic storm track is most active in summer unlike the midlatitude storm tracks of the North Atlantic and North Pacific, which are more active in winter months.

This seasonal peak in Arctic storm activity occurs exactly during the months in which human activity is increasing most rapidly, as melting sea ice opens shortened shipping routes between Europe and Asia as well as opportunities for tourism and industry (Eguíluz et al., 2016; Goessling et al., 2016). This is also the time of year when the sea ice is most vulnerable to fracture and decay, and cyclones have been linked to a number of recent rapid sea ice loss events (Kriegsmann & Brümmer, 2014; Simmonds & Rudeva, 2012), as well as extreme outgassing events of CO_2 from the Arctic Ocean (Mathis et al., 2012). Therefore, developing an understanding of the response of Arctic summer cyclones to climate change is an important step toward both mitigating the risks associated with human activity in the far north and understanding the Arctic's physical response to climate change.
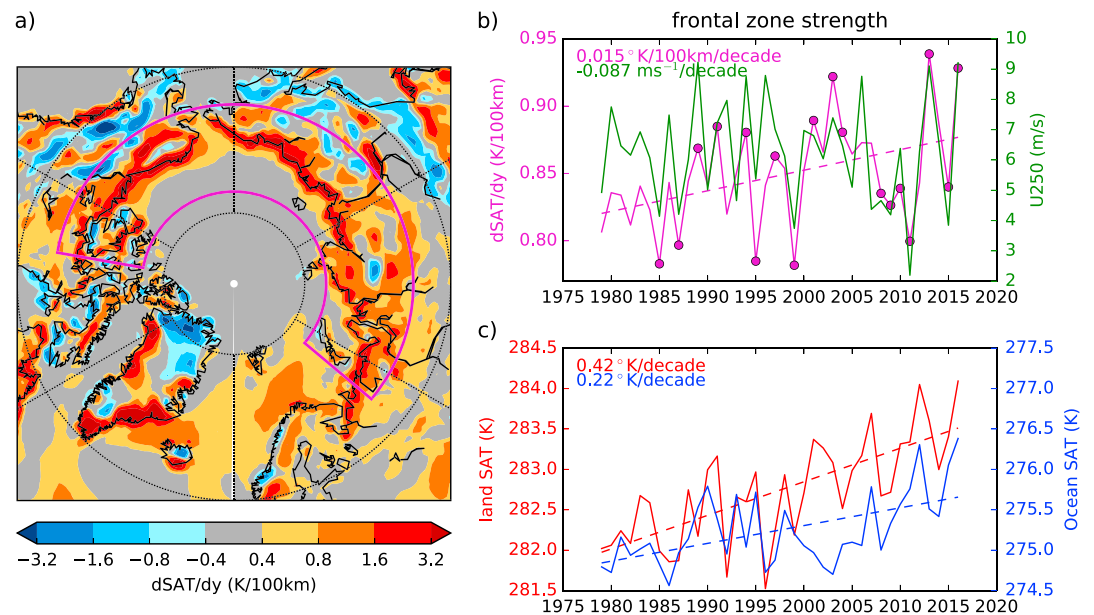
Figure 1. (a) Map of JJA mean equatorward 2 m temperature (SAT) gradients (with box illustrating the region referred to as the Arctic Frontal Zone, AFZ) . (b) Time series of area mean dSAT/dy within the AFZ (purple) and mean 300 hPa zonal wind over the Arctic (70 N–90 N) and (c) time series of 2 m temperature in the land and ocean sections of the AFZ. Dots indicate years in the highest and lowest quartiles of dSAT/dy within the AFZ. The linear trend in each time series is shown in each subfigure.

Previous observational studies have provided conflicting results for the question of whether Arctic summer storminess is increasing, with some finding that both frequency and intensity have significantly increased (Simmonds & Keay, 2009) and others find that they have not (Koyama et al., 2017), although these studies use different storm-tracking methodologies and deferent reanalyses. Evidence from climate model projections is more coherent, with models showing some significant increases in storminess, measured in various ways, by the end of the 21st century, which these studies argue is due to increasing baroclinicity in the AFZ (Crawford & Serreze, 2017; Day et al., 2018; Nishii, Nakamura, & Orsolini, 2014; Orsolini & Sorteberg, 2009). However, climate models perform poorly in reproducing even the basic characteristics of the present-day Arctic summer cyclone climatology (Day et al., 2018; Nishii et al., 2014), and so their projections of future change may not be reliable.

In this study an analog method is applied to bridge the gap between these observation and modeling-based studies. We perform a composite analysis of cyclone characteristics, of years with high and low temperature gradients, which we argue is a useful analog to climate change. This approach is not subject to some of the issues in previous work on this topic. A small signal-to-noise ratio is avoided by compositing over many years, in contrast to the analysis of trends. Further, the issue of model bias is minimized by using the ERA-Interim reanalysis (Dee et al., 2011), which is constrained by observations, in contrast to free-running Coupled Model Intercomparison Project (CMIP)-type projection studies.

2. Data and Methods

We performed a composite analysis on both seasonal mean fields and statistics of tracked cyclones using the ERA-Interim reanalysis. Composites were made for the highest and lowest quartile years (see Table S1 in the supporting information) of the AFZ index, defined as the mean equatorward 2 m temperature gradient in the AFZ (purple box in Figure 1a). This is similar to the index used in Day et al. (2018) and Nishii et al. (2014), although the northern boundary is defined slightly farther north than in these studies to better capture the full latitudinal extent of the AFZ in Siberia. Defining this index using 2 m temperatures, rather than upper level fields, also allows for direct comparison with observations (see supporting information).

Cyclones were tracked using the Hodges (1994, 1996, 1999) algorithm, which has been used extensively to study extratropical, and more recently Arctic cyclones, in both climate models and atmospheric reanalyses

(e.g., Bengtsson, Hodges, & Keenlyside, 2009; Day et al., 2018; Hodges, Lee, & Bengtsson, 2011; Zappa, Shaffrey, & Hodges, 2013).

In this algorithm, 850 hPa vorticity is computed from the 6-hourly zonal and meridional wind fields. The resulting vorticity field is then subjected to a number of preprocessing steps. First, it is spectrally filtered, retaining only wave numbers $5 < n \leq 42$, which removes small-scale and background features leaving only synoptic-scale phenomena. Spectral tapering is applied to the resultant field to suppress Gibbs phenomena, following Sardeshmukh and Hoskins (1984). Second, the filtered vorticity field is transformed onto a regular grid of similar resolution to the filtered data, in this case a polar stereographic projection. This prevents biases in cyclone identification at higher latitudes, caused by the converging of meridians when using, for example, a cylindrical projection (Sinclair, 1997). Grid point vorticity maxima in the filtered and projected vorticity that exceed a vorticity of 10^{-5} s^{-1} are those identified as cyclones. Their locations are then refined using a B-spline interpolation and steepest ascent method to compute the off-model-grid locations, which helps to produce smoother tracks (Hodges, 1994). Once the cyclone is identified, they are transformed back onto the spherical coordinate system for computing the actual tracks. A first-guess at the track is made by applying a nearest neighbor method to the vorticity maxima in adjacent time steps of the data, this is then refined iteratively by minimizing a cost function for the track smoothness, measured by changes in direction and speed, subject to adaptive constraints on track smoothness and displacement distance (Hodges, 1999), suitably chosen for the extra-tropics.

In a further step, tracks are filtered so that only the cyclone tracks that have a lifetime greater than 2 days and displacement distance of 1,000 km or more are retained for the final analysis. This avoids the inclusion of stationary and short-lived features, so that only well-defined cyclones are included. These filtering conditions have typically been used for midlatitude cyclones (e.g., Hodges et al., 2011). However, published case studies of Arctic synoptic scale cyclones indicate that these lifetime and propagation thresholds are suitable choices, since Arctic cyclones are typically longer lived than extratropical cyclones, and propagate similar distances (e.g., Aizawa & Tanaka, 2016; Simmonds & Rudeva, 2012; Tanaka, Yamagami, & Takahashi, 2012; Yamagami, Matsueda, & Tanaka, 2017).

Spatial statistics for the storm tracks, such as track density and propagation speeds are calculated using spherical kernel functions, as described in Hodges (1996). During our composite analysis, the statistical significance of anomalies in the spatial fields, between the highest and lowest AFZ index quartiles, employs the permutation track resampling method described in Hodges (2008). This is a Monte Carlo approach that randomly resamples the tracks repeatedly without replacement. In this case statistics were calculated from 2,000 replicates of the tracks to estimate the $p = 0.05$ level.

In order to investigate cyclone intensity, a number of additional fields are referenced to the storm tracks already described. The full resolution wind speed and vorticity are obtained for each track position by finding the maximum within a 6° radius. In the case of mean sea level pressure (MSLP), the minimum is determined within a 5° radius. Intensity histograms use the maximum/minimum value achieved by each track within the region of interest.

For all other analyses of the background state, monthly mean fields from ERA-Interim were used. The one exception being the Seasonally Varying-Northern Annular Mode (SV-NAM) index of Ogi et al. (2004), which was obtained from them directly, and calculated from the NCEP-NCAR reanalysis. The maximum Eady growth rate, shown in Figure 3, is calculated using monthly means, following the Hoskins and Valdes (1990) form: $\sigma = 0.31 f \left| \frac{\partial u}{\partial z} \right| N^{-1}$, where f is the Coriolis force, and N is the Brunt-Vaisala frequency. The vertical gradient in zonal wind is calculated from differences between adjacent vertical levels and interpolated to 850 hPa.

3. Results

3.1. Increasing Land-Sea Thermal Contrast

The magnitude of the area-mean 2 m temperature gradients in the AFZ (indicated by the purple box in Figure 1a) varies significantly from year to year, between 0.74–0.94 K/100 km, and has increased over time (Figure 1b), according to the ERA-Interim reanalysis. This year-to-year variability is significantly correlated

with 2 m temperature over the land surface ($r = 0.31$, $p = 0.05$), but not over the ocean ($r = -0.13$, $p = 0.44$). This indicates that although the ocean and land surface as well as atmospheric processes play a role in maintaining the climatology of surface temperature gradients, in this region, it is the processes affecting the land surface temperature that are the most important in driving the year-to-year variability. Variability in the AFZ strength is also highly correlated with the Arctic (70–90°N) zonal wind speed at 250 hPa (Figure 1b; $r = 0.73$, $p = 0.00$), as one would expect due to thermal wind balance arguments, indicating a strong relationship between surface properties and the large scale atmospheric circulation.

The upward trend in the strength of the AFZ temperature gradients occurs because the 2 m temperature trends over land are almost twice those over the ocean, in ERA-Interim (Figure 1c). This picture, from ERA-Interim, is consistent with in situ 2-m-land temperature and observed SST analyses for the region (Figure S1), giving independent confirmation that these trends are realistic. However, there is significant disagreement between the reanalyses: ERA-Interim (Dee et al., 2011), JRA-55 (Ebita et al., 2011) and MERRA2 (Gelaro et al., 2017) as to the magnitude of trends in the AFZ strength (See Figures S2 and S3). Nevertheless, enhanced land-sea temperature contrasts are a robust feature of both past and expected future climate change and ongoing warming of the Arctic is expected to lead to a further strengthening of temperature gradients in the AFZ.

Conveniently, the difference in the AFZ gradients between the highest and lowest years is within the range of the change expected by the end of the next century under business as usual emissions, -0.5–0.2 K/100 km, according to CMIP3 and 5 models (Day et al., 2018; Nishii et al., 2014). Therefore, comparing Arctic cyclone indices for high versus low-AFZ strength years will also provide direct observational evidence for how the Arctic summer storm track will respond to the more baroclinic coastal environment expected under climate change. A similar analog approach has been used to test hypotheses of the role of moist processes in the response of the North Atlantic storm track to climate change (Li et al., 2014).

3.2. Composite Analysis: Differences in Cyclone Statistics

With this in mind this study conducts a composite analysis of the circulation by comparing the JJA circulation for high and low strength AFZ years. These years are chosen by picking the highest and lowest quartiles based on the dT_{2m}/dy AFZ index shown in Figure 1b. Although the various reanalyses disagree over the trend in this index, they broadly agree over which years belong to each quartile (Table S1).

Years with strong gradients in the AFZ are characterized by significantly increased storm track densities in the Arctic (Figure 2c). This is particularly true in the Pacific Sector of the Arctic, including the Chukchi and Beaufort Sea, where track densities are almost double those in weak years.

Because there is no significant change in cyclone lifetime, we can attribute this change in density partly to an increase in the number of cyclones in the region, with increases of 11% from 16.3/month to 18.1/month (over the Arctic Ocean), but also to an increase in the coherence of trajectories, which tend to follow the Arctic coastline (see Figure S4). This suggests that the AFZ and associated jet acts as a wave guide for the cyclones during positive AFZ phases. In contrast, during years with a weak AFZ and jet the cyclones in the Arctic tend to meander and travel shorter distances (Figures S4b, S4d, and S4g).

One of the reasons for the increase in track density is a significant increase in cyclogenesis within the Arctic, particularly over the Pacific-side of the Arctic Ocean, where genesis events increase from 4.2/month to 5.6/month, and in the Greenland Sea (from 2.0/month to 2.7/month, Figure 2f). This increase in cyclogenesis goes hand in hand with an increase in baroclinic instability, as measured by the maximum Eady growth rate (Figure 2e; see section 2), which closely matches the zonal wind anomaly. This, suggests that an increase in shear instability is acting to increase storminess across the Arctic. However, increased static stability on the Pacific-side of the Arctic and reduced stability in the Atlantic-Arctic sector are acting to reduce and increase storminess, respectively (Figure S7b). An open question remains over the role of tropopause polar vortices, as precursors for Arctic cyclogenesis, in these year-to-year variations (Cavallo & Hakim, 2013).

Cyclogenesis has been observed in other studies, based on reanalyses, in this region, and these conclusions are slightly at odds with those of Crawford and Serreze (2016), who found that the AFZ was not an important zone for cyclogeneses. This may be because they defined the AFZ as a narrow band along the coastline, although they also use a different reanalysis and tracking scheme. Such a narrow band is likely not the best measure for investigating the interaction with the large scale, since the latitudinal position of the AFZ (whose
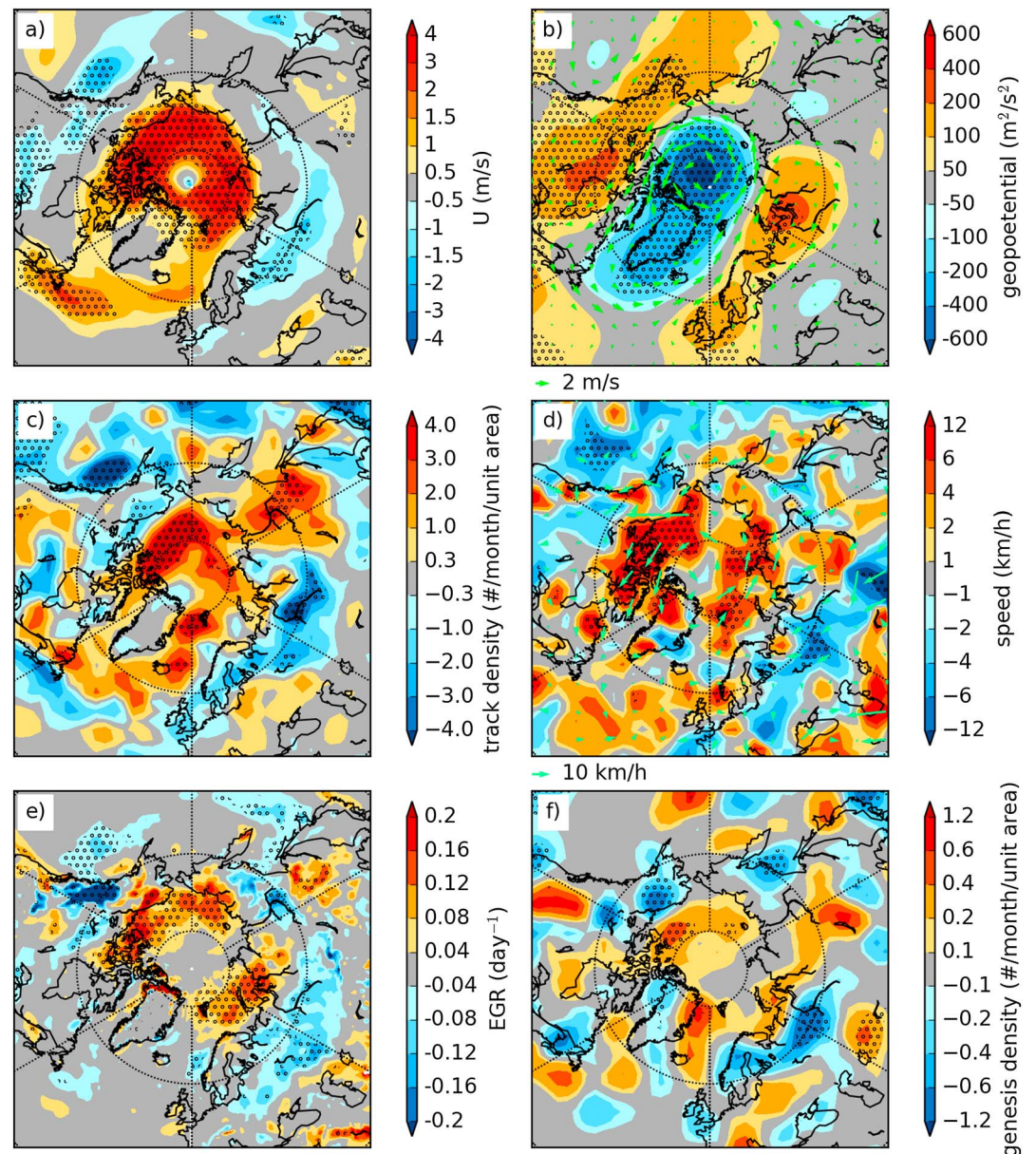
Figure 2. Differences between composites for high-low AFZ quartiles for (a) 850 hPa zonal wind, (b) 850 hPa geopotential (and wind vectors), (c) storm track density, (d) storm propagation speed (and vectors), (e) maximum Eady growth rate, and (f) genesis density. Stippling indicates regions where the differences are significant at the 5% level.

variability is shown by the black contour in Figure 3b), while closely tied to the Arctic coastline at the surface, varies significantly from year to year in the middle and upper troposphere and may have a dynamical influence at significant distances from the Arctic coastline.

The largest differences in both track density and cyclone intensity occur in the Pacific-side of the Arctic Ocean, with cyclone frequency increasing from 12.8/month to 14.3/month in this region (see Figure 2c). A consistent increase in dynamical intensity is also present here, with significant shifts (according to a Kolmogorov-Smirnov test), in the intensity histograms of maximum vorticity, minimum pressure, and maximum winds, toward higher intensities during high AFZ index years compared to low (Figure 3.). The changes in the MSLP histograms are particularly prominent, although a significant part of this change, ~5 hPa, can be explained by changes in the seasonal mean MSLP in the Arctic (see Figure S7).
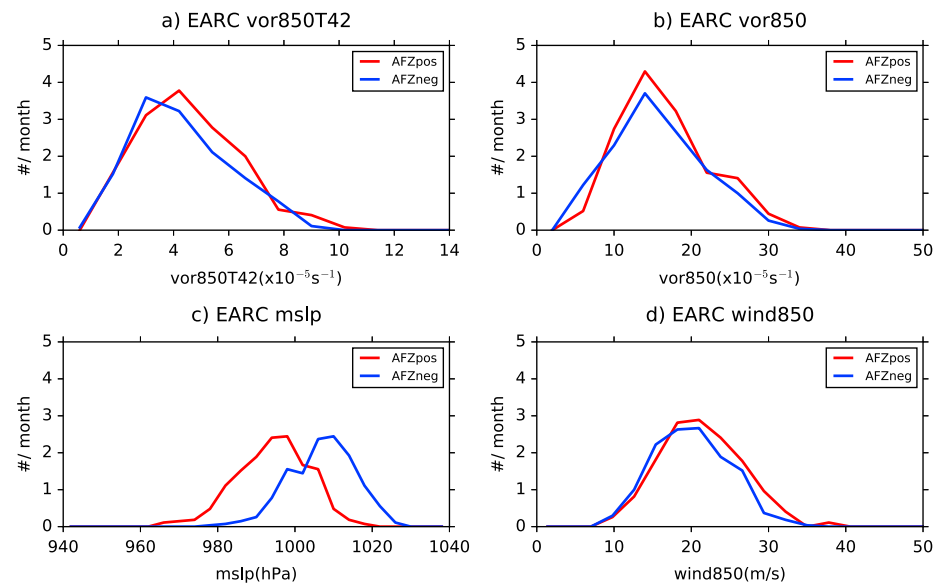
Figure 3. Histograms of cyclone intensity measures for the eastern Arctic Ocean (90–290°E, 72.5–90°N). In the case of maximum vorticity and winds the values correspond to the maximum value achieved by a storm within the region, for mslp it is the minimum value.

The propagation speed and velocity of the cyclones also increases significantly (Figure 2d) in a direction perpendicular to the coast, which is matched by the anomaly in the mean wind speeds, which are significantly higher in high AFZ conditions. This indicates that when a strong coastal temperature gradient exists, the Arctic Front Jet acts as a wave guide for cyclones along the Arctic coastline. Because the Arctic coastline closely matches the 70th parallel, the increased propagation is in a zonal direction along most longitudes. However, the North American coastline slopes southward from West to East; therefore, the acceleration of the flow leads to propagation of cyclones into lower latitudes over Eastern Canada and Baffin Bay toward the North Atlantic, increasing the flux of cyclones from high to lower latitudes, although the numbers of cyclones exiting the Arctic into the North Atlantic are in single figures.
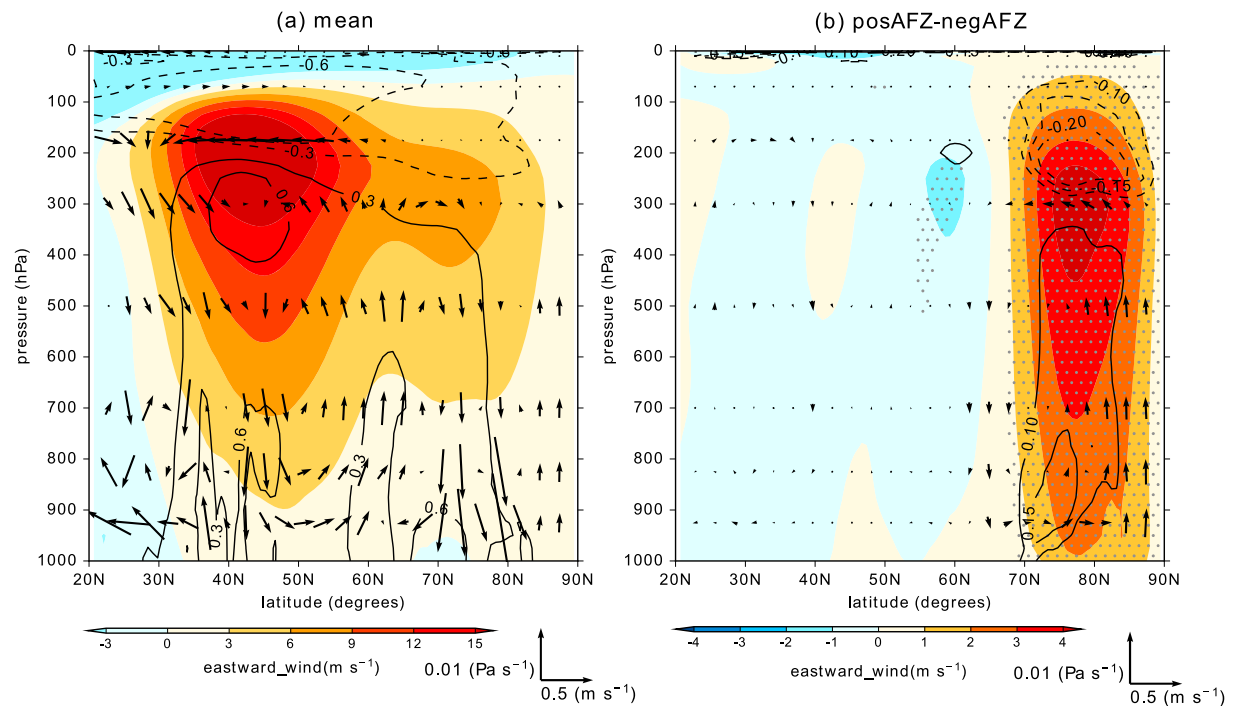
The changes in storminess suggested by this climate change analog are much larger than previous published estimates of the 21st century climate change from climate models, such as Day et al. (2018), who found no significant increase in track density in Arctic summer in the CESM1 model. Further, although the CMIP5 multimodel mean response is positive in the Arctic, it is an order of magnitude smaller than the response in this analog (Figure S6). However, a detailed investigation into the deficiencies in climate models will be needed to understand these issues.

4. Discussion: How Good Is this Analog?

Because significant differences exist in the large scale mean circulation between the high and low quartiles of the AFZ index, and these changes are clearly impacting the cyclone statistics, it is important to understand their origins and whether they play a role in the year-to-year variations in the strength of AFZ index itself.

The most positive quartile years are characterized by warm anomalies over land and cold anomalies over the Arctic Ocean, compared to the most negative quartile. These anomalies extend throughout the troposphere and correspond with a strengthening of the meridional temperature gradients on the oceanward side of the Arctic coastline (Figure 2b). As one would expect from the thermal wind relationship, they correspond with a strengthened jet, which is as much as 5 m/s faster, with positive zonal wind anomalies extending through the Arctic troposphere around the Arctic basin (Figures 2 and 4a). A meridional overturning cell, north of the Arctic Front and similar to that described by Shapiro, Hampel, and Krueger (1987), is present in the climatology (Figure 2a), and the composite anomalies show a clear strengthening of this circulation with increased upwelling on the poleward flank of the Arctic Front Jet and downwelling on the equatorward side in years with a strong AFZ. As well as a strengthening of the Arctic Jet, the jet center is also shifted northward in

Figure 4. Cross sections of zonal mean zonal wind (contours), meridional and vertical wind components (vectors), and meridional temperature gradients (contour labels are in K/100 km) for JJA mean (a) and difference between the composite means of highest and lowest Arctic Frontal Zone quartiles (b). Stippling shows regions where the anomaly is significant at the $p = 0.05$ level.

positive years. This goes hand in hand with a northward expansion of the baroclinic zone, in the mid-upper troposphere, from the Arctic coastline over the central Arctic Ocean (Figure 4b).

The geopotential height anomaly is highly reminiscent of the summer NAM and the correlation between the AFZ index and the SV-NAM index of Ogi et al. (2004) is highly significant at 0.54. Further, the Arctic (70–90°N) zonal mean wind at 300 hPa is highly correlated with the AFZ index ($r = 0.70$), indicating a strong link between the AFZ index and the zonal mean circulation. This is a clear indication that the storm track and thermally driven jet, associated with the AFZ, are really dominant over external influences in this region. Therefore, it seems likely that changes in the AFZ and local baroclinicity will dominate over lower-latitude influences in determining the response of Arctic cyclones to climate change.

A mechanism to explain this link between the upper tropospheric winds and surface baroclinicity is found through analysis of radiative fluxes at the surface. Anomalous zonal winds above the Arctic during high AFZ years occur concurrently with negative anomalies in vertical velocity in a band 60–70°N (see Figure S5). Reduced adiabatic cooling in this situation and anomalously low cloud cover results in an increase of downwelling shortwave radiation and increased temperatures over land. The opposite pattern is seen over the Arctic Ocean, where anomalously large vertical velocities lead to increased cloud cover, a reduction in downwelling shortwave, which results in anomalously cold temperatures and increased sea ice concentration. Note that a 4 W/m² difference in shortwave radiation corresponds to approximately 17 cm of sea ice melt. In this way NAM-related variations in circulation patterns can influence near-surface baroclinicity.

As the NAM is a largely internal mode of atmospheric variability, it is likely that much of the year-to-year variability in the AFZ index is also internally generated. However, external forcing from volcanoes and solar variability play a significant role in driving year-to-year temperature variability in high latitudes (Smith et al., 2012), and therefore also likely play a role in variability of the AFZ index. Nevertheless, the fact that year-to-year variations in the AFZ index are linked to the NAM should not be seen as a weakness of these composites as an analog for climate change since climate models broadly agree that the response of Northern Hemisphere circulation to climate change will be positive-NAM-like with reduced zonal winds at low latitudes and increased zonal winds at high latitudes (Coumou et al., 2015; Day et al., 2018; Mann et al., 2017).

5. Conclusions

In this study we have investigated near-surface air temperature gradients along the Arctic coastline in a number of reanalysis products and observations and constructed an index for coastal baroclinicity (the AFZ index). We have used this to construct an analog for future climate change using the highest and lowest quartile years of this index as an analog for climate change and performed composite analysis of atmospheric fields, to infer the response of Arctic cylones to climate change.

In summary, we observed

1. that 2 m land temperatures near the Arctic coastline are warming at approximately twice the rate of sea surface temperatures in adjacent regions;
2. that significantly increased Arctic cyclone frequency and intensity, particularly in the Eastern part of the Arctic Ocean, are characteristic of years with high Arctic coastal temperature gradients, compared to low years; and
3. that the sign of this response is consistent with climate model projections, but the magnitude of change in cyclone numbers is higher, suggesting that CMIP models underestimate the sensitivity of the summer storm track to increasing land-sea contrast in the Arctic.

Further, because climate change is increasing land-sea contrasts in the Arctic, it seems highly likely that the circulation patterns typical of years with strong AFZ will become more common as the climate warms. Indeed, strengthening of the mean temperature gradients in the AFZ is a robust feature of future climate projections as is an increase in the strength of the Arctic Front Jet (Mann et al., 2017; Nishii et al., 2014). This study shows that this linkage between surface temperature gradients and atmospheric circulation is important for Arctic cyclones, adding weight to previous studies.

The discrepancy between different reanalysis products in terms of 2 m temperature trends in the AFZ (Figures 1, S1, and S2) indicates significant shortcomings in the performance of some reanalyses in the Arctic. Therefore, understanding the thermodynamic processes involved in maintaining the AFZ and improving their representation in numerical models, and reanalysis, should be seen as an important step in improving simulations of the atmosphere both in the Arctic and beyond.

References

Aizawa, T., & Tanaka, H. L. (2016). Axisymmetric structure of the long lasting summer Arctic cyclones. *Polar Science*, *10*(3), 192–198. https://doi.org/10.1016/j.polar.2016.02.002

Bengtsson, L., Hodges, K. I., & Keenlyside, N. (2009). Will extratropical storms intensify in a warmer climate? *Journal of Climate*, *22*(9), 2276–2301. https://doi.org/10.1175/2008JCLI2678.1

Cavallo, S. M., & Hakim, G. J. (2013). Physical mechanisms of tropopause polar vortex intensity change. *Journal of the Atmospheric Sciences*, *70*(11), 3359–3373. https://doi.org/10.1175/JAS-D-13-088.1

Coumou, D., Lehmann, J., & Beckmann, J. (2015). The weakening summer circulation in the Northern Hemisphere mid-latitudes. *Science*, *348*(6232), 324–327. https://doi.org/10.1126/science.1261768

Crawford, A. D., & Serreze, M. C. (2014). A new look at the summer Arctic frontal zone. *Journal of Climate*, *28*(2), 737–754. https://doi.org/10.1175/JCLI-D-14-00447.1

Crawford, A. D., & Serreze, M. C. (2016). Does the summer Arctic frontal zone influence Arctic Ocean cyclone activity? *Journal of Climate*, *29*(13), 4977–4993. https://doi.org/10.1175/JCLI-D-15-0755.1

Crawford, A. D., & Serreze, M. C. (2017). Projected changes in the Arctic frontal zone and summer Arctic cyclone activity in the CESM large ensemble. *Journal of Climate*, *30*(24), 9847–9869. https://doi.org/10.1175/JCLI-D-17-0296.1

Day, J. J., Holland, M. M., & Hodges, K. I. (2018). Seasonal differences in the response of Arctic cyclones to climate change in CESM1. *Climate Dynamics*, *50*, 3885. https://doi.org/10.1007/s00382-017-3767-x

Dee, D. P., Uppala, S. M., Simmons, A. J., Berrisford, P., Poli, P., Kobayashi, S., et al. (2011). The ERA-interim reanalysis: Configuration and performance of the data assimilation system. *Quarterly Journal of the Royal Meteorological Society*, *137*(656), 553–597. https://doi.org/10.1002/qj.828

Ebita, A., Kobayashi, S., Ota, Y., Moriya, M., Kumabe, R., Onogi, K., et al. (2011). The Japanese 55-year reanalysis "JRA-55": An interim report. *Solaiat*, *7*, 149–152. https://doi.org/10.2151/sola.2011-038

Eguíluz, V. M., Fernández-Gracia, J., Irigoien, X., & Duarte, C. M. (2016). A quantitative assessment of Arctic shipping in 2010–2014. *Scientific Reports*, *6*(1). https://doi.org/10.1038/srep30682

Gelaro, R., McCarty, W., Suárez, M. J., Todling, R., Molod, A., Takacs, L., et al. (2017). The modern-era retrospective analysis for research and applications, version 2 (MERRA-2). *Journal of Climate*, *30*(14), 5419–5454. https://doi.org/10.1175/JCLI-D-16-0758.1

Goessling, H. F., Jung, T., Klebe, S., Baeseman, J., Bauer, P., Chen, P., et al. (2016). Paving the way for the year of polar prediction. *Bulletin of the American Meteorological Society*, *97*(4), ES85–ES88. https://doi.org/10.1175/BAMS-D-15-00270.1

Hodges, K. I. (1994). A general method for tracking analysis and its application to meteorological data. *Monthly Weather Review*, *122*(11), 2573–2586. https://doi.org/10.1175/1520-0493(1994)122%3C2573:AGMFTA%3E2.0.CO;2

Hodges, K. I. (1996). Spherical nonparametric estimators applied to the UGAMP model integration for AMIP. *Monthly Weather Review*, *124*(12), 2914–2932. https://doi.org/10.1175/1520-0493(1996)124%3C2914:SNEATT%3E2.0.CO;2

Hodges, K. I. (1999). Adaptive constraints for feature tracking. *Monthly Weather Review*, *127*(6), 1362–1373. https://doi.org/10.1175/1520-0493(1999)127%3C1362:ACFFT%3E2.0.CO;2

Hodges, K. I. (2008). Confidence intervals and significance tests for spherical data derived from feature tracking. *Monthly Weather Review*, *136*(5), 1758–1777. https://doi.org/10.1175/2007MWR2299.1

Hodges, K. I., Lee, R. W., & Bengtsson, L. (2011). A comparison of extratropical cyclones in recent reanalyses ERA-interim, NASA MERRA, NCEP CFSR, and JRA-25. *Journal of Climate*, *24*(18), 4888–4906. https://doi.org/10.1175/2011JCLI4097.1

Hoskins, B. J., & Valdes, P. J. (1990). On the existence of storm-tracks. *Journal of the Atmospheric Sciences*, *47*(15), 1854–1864. https://doi.org/10.1175/1520-0469(1990)047%3C1854:OTEOST%3E2.0.CO;2

Koyama, T., Stroeve, J., Cassano, J., & Crawford, A. (2017). Sea ice loss and Arctic cyclone activity from 1979 to 2014. *Journal of Climate*, *30*(12), 4735–4754. https://doi.org/10.1175/JCLI-D-16-0542.1

Kriegsmann, A., & Brümmer, B. (2014). Cyclone impact on sea ice in the Central Arctic Ocean: A statistical study. *The Cryosphere*, *8*(1), 303–317. https://doi.org/10.5194/tc-8-303-2014

Li, M., Woollings, T., Hodges, K., & Masato, G. (2014). Extratropical cyclones in a warmer, moister climate: A recent Atlantic analogue. *Geophysical Research Letters*, *41*(23), 8594–8601. https://doi.org/10.1002/2014GL062186

Mann, M. E., Rahmstorf, S., Kornhuber, K., Steinman, B. A., Miller, S. K., & Coumou, D. (2017). Influence of anthropogenic climate change on planetary wave resonance and extreme weather events. *Scientific Reports*, *7*, 45242. https://doi.org/10.1038/srep45242

Mathis, J. T., Pickart, R. S., Byrne, R. H., McNeil, C. L., Moore, G. W. K., Juranek, L. W., et al. (2012). Storm-induced upwelling of high pCO$_2$ waters onto the continental shelf of the western Arctic Ocean and implications for carbonate mineral saturation states. *Geophysical Research Letters*, *39*, L07606. https://doi.org/10.1029/2012GL051574

Nishii, K., Nakamura, H., & Orsolini, Y. J. (2014). Arctic summer storm track in CMIP3/5 climate models. *Climate Dynamics*, *44*(5-6), 1311–1327. https://doi.org/10.1007/s00382-014-2229-y

Ogi, M., Yamazaki, K., & Tachibana, Y. (2004). The summertime annular mode in the Northern Hemisphere and its linkage to the winter mode. *Journal of Geophysical Research*, *109*, D20114. https://doi.org/10.1029/2004JD004514

Orsolini, Y. J., & Sorteberg, A. (2009). Projected changes in Eurasian and Arctic summer cyclones under global warming in the Bergen climate model. *Atmospheric and Oceanic Science Letters*, *60*(3), 557–569. https://doi.org/10.1111/j.1600-0870.2008.00305.x

Reed, R. J., & Kunkel, B. A. (1960). The Arctic circulation in summer. *Journal of Meteorology*, *17*(5), 489–506. https://doi.org/10.1175/1520-0469(1960)017%3C0489:TACIS%3E2.0.CO;2

Sardeshmukh, P. D., & Hoskins, B. I. (1984). Spatial smoothing on the sphere. *Monthly Weather Review*, *112*(12), 2524–2529. https://doi.org/10.1175/1520-0493(1984)112%3C2524:SSOTS%3E2.0.CO;2

Serreze, M. C. (1995). Climatological aspects of cyclone development and decay in the Arctic. *Atmosphere-Ocean*, *33*(1), 1–23. https://doi.org/10.1080/07055900.1995.9649522

Serreze, M. C., & Barrett, A. P. (2008). The summer cyclone maximum over the Central Arctic Ocean. *Journal of Climate*, *21*(5), 1048–1065. https://doi.org/10.1175/2007JCLI1810.1

Serreze, M. C., Lynch, A. H., & Clark, M. P. (2001). The Arctic frontal zone as seen in the NCEP–NCAR reanalysis. *Journal of Climate*, *14*(7), 1550–1567. https://doi.org/10.1175/1520-0442(2001)014%3C1550:TAFZAS%3E2.0.CO;2

Shapiro, M. A., Hampel, T., & Krueger, A. J. (1987). The Arctic tropopause fold. *Monthly Weather Review*, *115*(2), 444–454. https://doi.org/10.1175/1520-0493(1987)115%3C0444:TATF%3E2.0.CO;2

Simmonds, I., & Keay, K. (2009). Extraordinary September Arctic sea ice reductions and their relationships with storm behavior over 1979–2008. *Geophysical Research Letters*, *36*, L19715. https://doi.org/10.1029/2009GL039810

Simmonds, I., & Rudeva, I. (2012). The great Arctic cyclone of August 2012. *Geophysical Research Letters*, *39*, L23709. https://doi.org/10.1029/2012GL054259

Sinclair, M. R. (1997). Objective identification of cyclones and their circulation intensity, and climatology. *Weather and Forecasting*, *12*(3), 595–612. https://doi.org/10.1175/1520-0434(1997)012%3C0595:OIOCAT%3E2.0.CO;2

Smith, D. M., Scaife, A. A., & Kirtman, B. P. (2012). What is the current state of scientific knowledge with regard to seasonal and decadal forecasting? *Environmental Research Letters*, *7*(1), 15602. https://doi.org/10.1088/1748-9326/7/1/015602

Tanaka, H. L., Yamagami, A., & Takahashi, S. (2012). The structure and behavior of the Arctic cyclone in summer analyzed by the JRA-25/JCDAS data. *Polar Science*, *6*(1), 55–69. https://doi.org/10.1016/j.polar.2012.03.001

Yamagami, A., Matsueda, M., & Tanaka, H. L. (2017). Extreme Arctic cyclone in August 2016. *Atmospheric Science Letters*, *18*(7), 307–314. https://doi.org/10.1002/asl.757

Zappa, G., Shaffrey, L. C., & Hodges, K. I. (2013). The ability of CMIP5 models to simulate North Atlantic extratropical cyclones*. *Journal of Climate*, *26*(15), 5379–5396. https://doi.org/10.1175/JCLI-D-12-00501.1